Electrodynamic constraints on homogeneity and RF power deposition in multiple coil excitations

R. Lattanzi[1,2], D. K. Sodickson[3], A. K. Grant[2,4], and Y. Zhu[5]

[1]Division of Health Sciences and Technology, Harvard-MIT, Cambridge, MA, United States, [2]Beth Israel Deaconess Medical Center, Boston, MA, United States, [3]New York University Medical Center, New York, NY, United States, [4]Harvard Medical School, Boston, MA, United States, [5]GE Global Research, Niskayuna, NY, United States

Introduction

Correction of B_1 inhomogeneities and management of SAR are among the most difficult challenges faced by *in-vivo* ultra high field MR applications. The use of multiple independently driven transmit elements, which enables fine control over the distribution of electromagnetic fields, has been explored as a possible solution and various approaches have been developed. In parallel transmission techniques [1,2] the composite B_1 field can be modulated in space and time by adjusting the independent RF waveforms transmitted by each coil, in order to generate a target excitation profile while minimizing SAR [2]. There are inherent limitations to this dual optimization process, which were described at a recent conference [3] for a uniform spherical sample. In this work we propose a different electrodynamic formulation for the calculation of ultimate intrinsic SAR, which enables derivation of the corresponding optimal current patterns on the surface of the sphere. The trade-off between transmit homogeneity and SAR reduction was investigated using this formulation, and the behavior of ideal current patterns was studied.

Theory and Methods

The RF power dissipated in the patient over an excitation can be expressed as a quadratic function in the samples of the current waveforms $\mathbf{I}_p$: $\xi = 1/P\sum_1^P 1/2\int_V \sigma(\mathbf{r})\left|E(\mathbf{r},p\Delta t)\right|^2 d\mathbf{r} = 1/P\sum_1^P(\mathbf{I}_p^H \mathbf{\Phi}\mathbf{I}_p)$, where σ is the tissue conductivity, E is a linear combination of the electric fields generated by the elements of the transmit array, Δt is the length of each sampling interval, P is the total number of samples and $\mathbf{\Phi}$ is a positive definite covariance matrix given by $\Phi_{i,j} = \int_V \sigma(\mathbf{r})e_j^*(\mathbf{r},t)\cdot e_i(\mathbf{r},t)d\mathbf{r}$ (with $e_i(\mathbf{r},t)$ the electric field generated by a unit current on the ith coil). In the case of a rectilinear EPI-based trajectory in excitation k-space, ξ can be related, using Parseval's theorem, to the periodic patterns $\mathbf{f}_n$ that define the excitation profile at each spatial position n [2]: $\xi = 1/N\sum_1^N(\mathbf{f}_n^H\mathbf{\Phi}\mathbf{f}_n)$. In parallel transmission the individual coil's current patterns are adjusted at each time point to correct excitation inhomogeneity voxel-by-voxel, resulting in a different set $\mathbf{f}_n$ for each of the N voxels. Among the possible $\mathbf{f}_n$, those that minimize ξ are given by [4]: $\tilde{\mathbf{f}}_n = \mathbf{\Phi}^{-1}\mathbf{C}_n^H(\mathbf{C}_n\mathbf{\Phi}^{-1}\mathbf{C}_n^H)^{-1}\mu_n$, where μ_n is the target profile and $\mathbf{C}_n$ contains the spatial weighting induced by the B_{1+} fields of each coil. The actual excited profile obtained with the minimum SAR pulse can be calculated as $\tilde{\mu}_n = \mathbf{C}_n\tilde{\mathbf{f}}_n$. A similar formulation applies when a single RF current source is used to drive all transmit coils, after being independently modulated in phase and amplitude for each channel. In this approach, known as RF shimming, there is a common excitation pattern and the optimization is performed only on the modulation coefficients. In order to find the theoretical lower bound of SAR, we defined a complete basis set of spherical surface current densities, including both magnetic and electric dipole densities, [5] and for each mode we calculated the electromagnetic field using the dyadic Green's function method [6]. SAR minimization was then performed using basis functions as elements of a hypothetical transmit array. The modes' electric and magnetic fields were used to calculate $\mathbf{\Phi}$ and the B_{1+} values in $\mathbf{C}_n$, respectively. The $\tilde{\mathbf{f}}_n^{ult}$ resulting in the ultimate intrinsic SAR were used to weight the current basis functions and find the corresponding optimal current patterns on the surface of the sphere. The algorithm was implemented on a standard PC using MATLAB (Mathworks, Natick, USA). Calculations were performed for different sphere radii, target excitation profiles, field strengths and acceleration factors. The electromagnetic properties of the material were chosen as in a previous study [7].

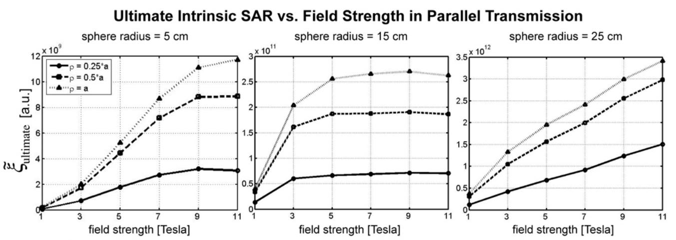

Fig. 1 Ultimate intrinsic average SAR for a transverse FOV through the center of a homogeneous sphere as a function of main magnetic field strength. The sphere electrical properties were modeled with frequency dependent average *in-vivo* values. Each column refers to a different size of the sphere. Plots are shown for 3 fully homogeneous concentric excitation profiles with radius equal to 100% (top curve), 50% (middle curve) and 25% (bottom curve) of the radius of the sphere *a*.

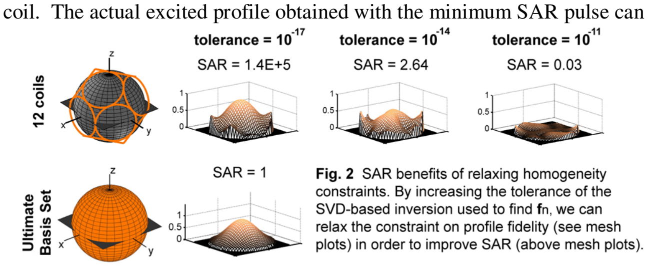

Fig. 2 SAR benefits of relaxing homogeneity constraints. By increasing the tolerance of the SVD-based inversion used to find **f**n, we can relax the constraint on profile fidelity (see mesh plots) in order to improve SAR (above mesh plots).

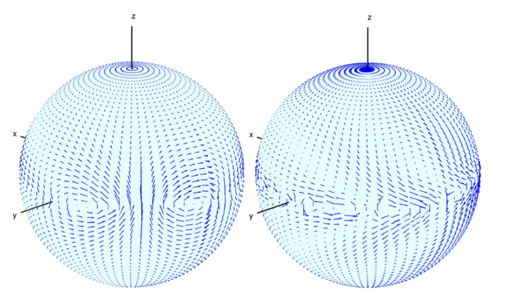

Fig. 3 Ideal surface current patterns resulting in the excitation of a fully homogeneous profile on a transverse slice through the center of the sphere, with the lowest possible SAR, in the case of Bo = 1.5T (left) and Bo = 7T (right). The ideal current is evaluated at every arrow position as the sum of the current modes, weighted with the optimal coefficients from parallel transmission. Each plot is a temporal snapshot of the real component of the current patterns at the center of excitation k-space.

Results and Discussion

Figure 1 shows ultimate intrinsic SAR as a function of main magnetic field strength, for the case of parallel transmission. Results are presented for various sphere radii (5cm, 15cm, 25cm from left to right) and for three fully homogeneous concentric excitation profiles. For a sphere radius of 15 cm there is an evident flattening in the growth of SAR with field strength, which can be explained by the relative scaling between the electric and magnetic field and by the controlled field cancellation, allowed when the wavelength becomes compatible with spatial focusing. Parallel transmission resulted in good homogeneity even using arrays with a limited number of transmit elements. Using RF shimming, inhomogeneities in the actual excited profile can be corrected either by using large arrays or by paying a high SAR price (Figure 2). The choice of the array geometry is important as in the end RF power deposition is governed by the current distribution produced by the transmit coils. Figure 3 shows a temporal snapshot of the ideal net current patterns (made up of optimally-weighted basis currents) in the case of unaccelerated parallel excitation of a fully homogeneous profile along the x-y plane. Distributed current loops dominate the behavior at 1.5T magnetic field strength (left), whereas the patterns become more complex at 7T (right).

Conclusions

We have described a theoretical framework for calculating the lowest possible SAR and the corresponding optimal current patterns in the case of parallel transmission and RF shimming. For parallel transmission, the flattening of the variation of ultimate intrinsic SAR with field strength suggests potential benefits of the technique for ultra-high field imaging. The same framework can be used in the case of finite transmit arrays to obtain the desired trade-off between B_1 homogeneity correction and RF power deposition, and this framework may also be used to measure practical array performance against ultimate limits. Ideal current patterns reflect the increasingly complex electrodynamics associated with RF transmission at increasing field strength. Knowledge of these optimal current patterns will serve as an important guide for future high-field coil designs compatible with high homogeneity and low SAR.

References

[1] Katscher U et al, (2003) MRM 49:144-150 [2] Zhu Y, (2004) MRM 51:775-784 [3] Lattanzi R et al, ISMRM 2007, 675 [4] Zhu Y, ISMRM 2006, 599 [5] Schnell W et al, (2000) IEEE Trans Ant Prop 48:418-28 [6] Tai CT, Dyadic Green Functions in Electromagnetic Theory (1994) [7] Wiesinger F et al (2004), MRM 52:953-964